ON THE REALITY OF MAGNETIC FINE STRUCTURE

CONSTANCE SAWYER

Space Disturbances Laboratory, ESSA Research Laboratories, Boulder, Colo. 80302, U.S.A.

On filter magnetograms of the Sun made at Lockheed Solar Observatory, small mottles create a salt-and-pepper appearance. Outside plages, the surface seems to be sprinkled with little magnetic elements, with opposite polarities intermingled. The many steps of the photographic subtraction process required to make these elements visible tend to cast doubt on their reality. Independent and stronger evidence for the quantization of magnetic field, recently presented by Livingston and Harvey (1969), stimulates an effort to define more carefully the characteristics of the elements seen on filter magnetograms. The purpose of this contribution is to show that these characteristics are compatible with those of the elements observed at Kitt Peak.

If one accepts the reality of the elements on the basis of the Kitt Peak observations, the Lockheed data offer a complementary view that may help us to use this new phenomenon to understand the development and decay of active regions.

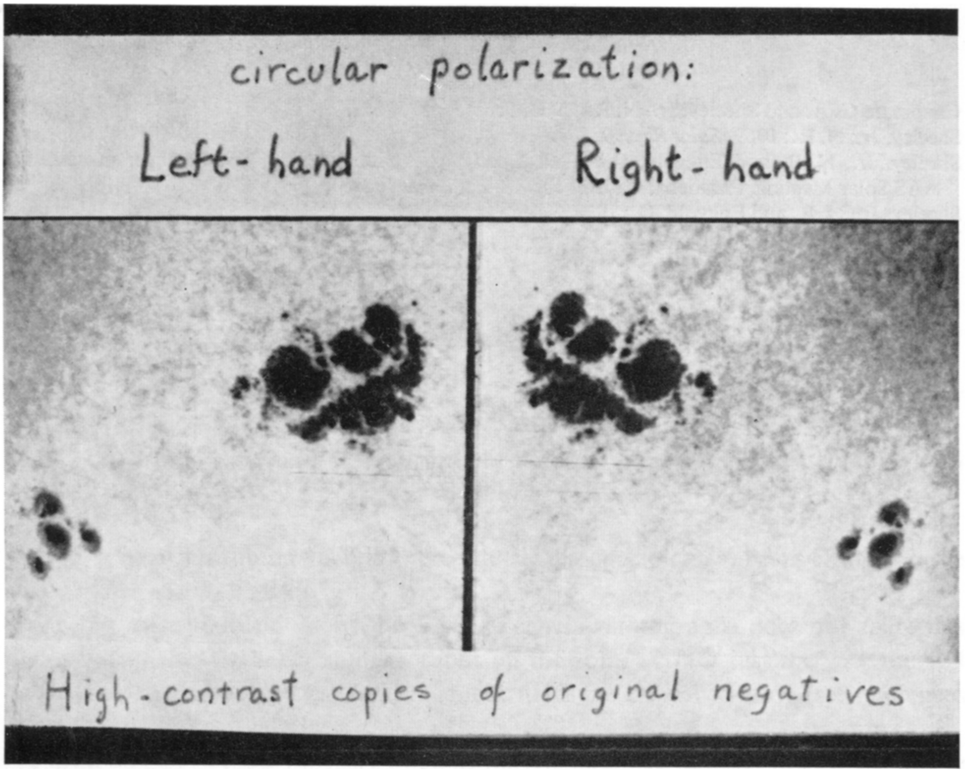

Fig. 1. High contrast copies of original negatives with opposite circular polarization.

Howard (ed.), Solar Magnetic Fields, 316–322.

The Lockheed filter transmits a 0.15 Å band in the blue wing of the half-Ångstrom broad, Zeeman-sensitive Fe I line at λ5324. A quarterwave plate is rotated between successive exposures of the solar image, so that right-hand circularly polarized light is recorded on one frame, and left-hand on the next. The resulting photographs (Figure 1) show sunspots, facular lanes, and fine structure, with rather subtle differences resulting from the polarization switch between neighboring frames. These differences are enhanced, and intensity variations that do not depend on polarization are suppressed, by photographic subtraction, which combines a positive image in each

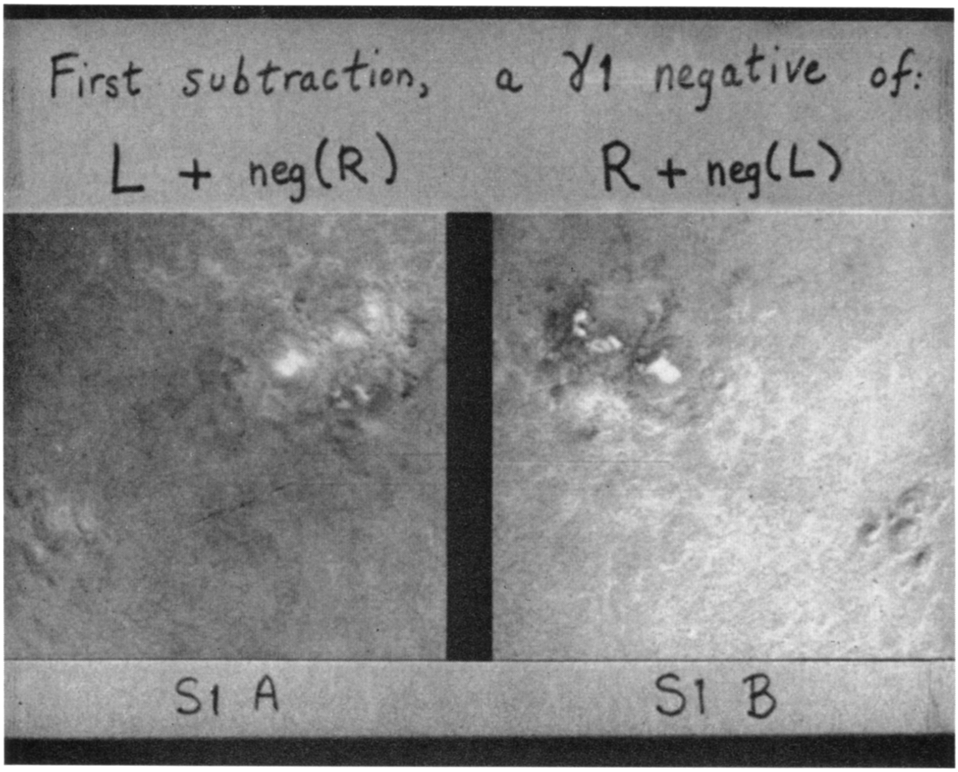

Fig. 2. First subtraction: the positive of one circular polarization is combined with the negative of the opposite polarization.

polarization with a negative image in the opposite polarization. The material studied here was prepared at Lockheed Observatory by carrying out two subtractions for each polarity, (Figures 2 and 3) making a half-tone print of each, and copying these on transparencies of different color. The part of the solar intensity field that is enhanced by a positive longitudinal magnetic field appears as high density on a red transparency, and the part enhanced by negative field as high density on a blue transparency. When these are overlayed, the strong fields in an active region stand out as intensely colored, coarsely structured regions, while outside the active region,

https://doi.org/10.1017/S0074180900022750 Published online by Cambridge University Press

the pattern consists of a mixture of red and blue dots that tend to form narrow meandering strings. The lanes that stand out most clearly look like network cell boundaries and are the same size.

The observations were made April 1, 1969, and show McMath plage 10014, with Mt. Wilson sunspot groups 17207 and 17211; lat ~N20, CMP about April 3.

The red and blue dots are complementary, in that dense dots on the red transparency overlie blank spots on the blue transparency, and vice versa. This gives a pronounced moiré effect when the transparencies are rotated slightly from exact super-

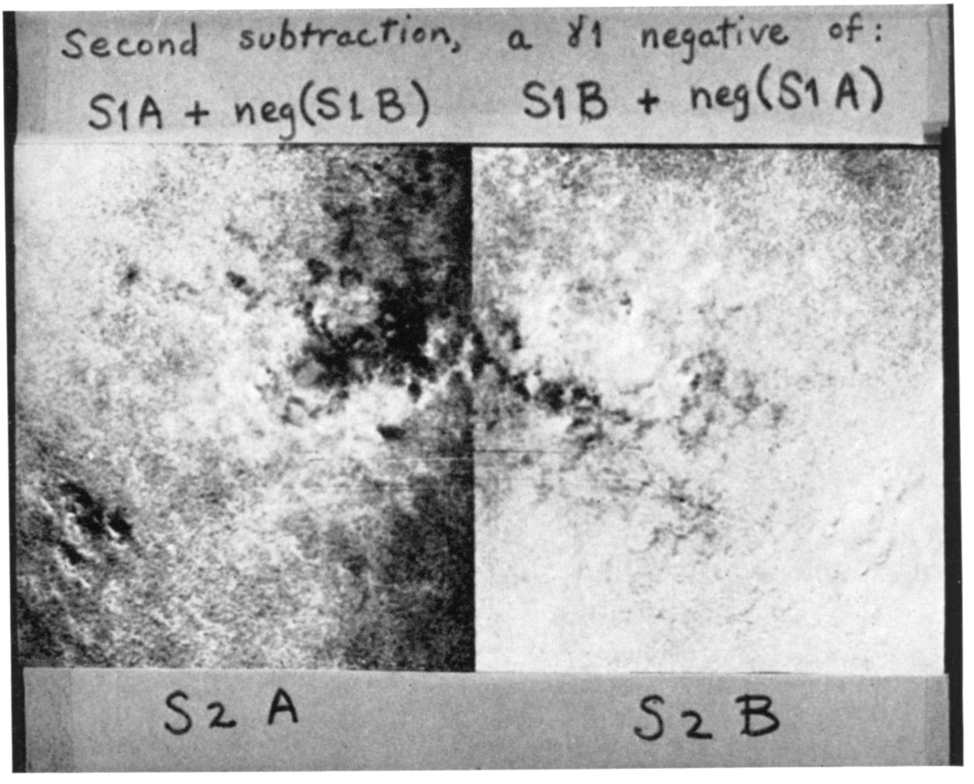

Fig. 3. Second subtraction: one first subtraction (Figure 2) is combined with the negative of the other first subtraction.

position. This effect is distinct from the moiré pattern produced from the half-tone grid. The grids on the two transparencies are at about 45° to each other, so that the half-tone moiré pattern appears when the transparencies are rotated through an angle of 45° from superposition. The 'magnetic dots' are much larger than the half-tone dots, by a factor of 8 or 10, and also considerably larger than the grain of the photographic emulsion. They are smaller than the mottles that can be seen before subtraction. In the various steps of the photographic process, the magnetic dots first become prominent (compared to the emulsion grain, for example) after the first subtraction.

The smallest dot that can be recognized on these prints includes four half-tone dots, an area of 1.25 (arc s)^2. Only one out of 6 dots are larger than 3 (arc s)^2, and many of these large dots are irregularly shaped and could well be clusters of individual dots. The mean area for 153 dots is 2.05 (arc s)^2, corresponding to a diameter of 1.″8 (an upper limit, because of the clustering and limited spatial resolution). The frequency distribution of dot area can be represented by an exponential relation:

$$-\ln\frac{N}{No} = \frac{\text{element area in (arc s)}^2}{1.2} = \frac{\text{area in } 10^6 \text{ km}^2}{0.6}.$$

Red dots and blue dots were counted in areas of about the same size as the Mount Wilson magnetograph aperture (275 (arc s)^2), and the corresponding magnetic field measure, ranging from less than 5 G up to 80 G, was found from the published Mount Wilson magnetogram (*Solar-Geophysical Data*). The signed difference, (number of red dots – number of blue dots), is correlated with the magnetic field, with correlation coefficient 0.90 (39 pairs of values) and regression relation close to:

$$\text{one uncompensated dot/aperture} = \text{one gauss}.$$

The *total* number of dots, red + blue, in each area is also related to the field, with

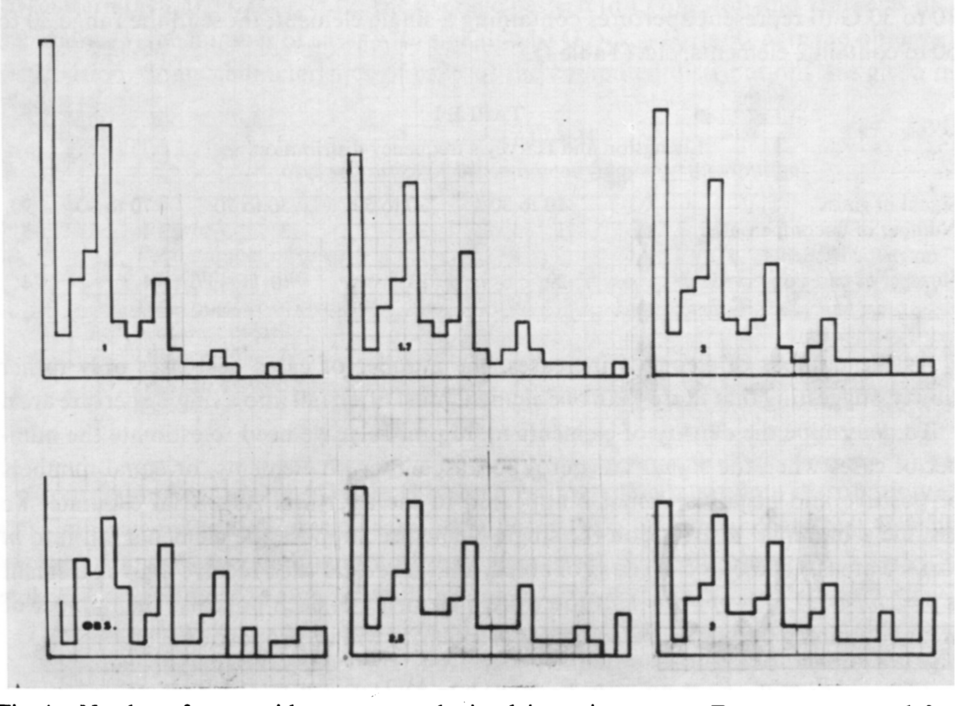

Fig. 4. Number of cases with magnetograph signal in a given range. Top row: computed for $x = np/q = 1$, 1.7, 2. Bottom row: the distribution observed by Livingston and Harvey (1969), computed for $x = 2.5$, $x = 3$.

correlation coefficient 0.69. This reflects the higher density of dots in plage regions.

The relation: 1 dot/aperture = 1 G, with the Mount Wilson aperture area of 275 (arc s)^2 = 1.45×10^{18} cm^2, leads to a value for the flux per dot of 1.4×10^{18} Mx. Temperature sensitivity of the line λ5250 used for the Mount Wilson measurements leads to underestimation of the flux by a factor of 2 or 3 (Harvey and Livingston, 1969), so a more realistic estimate of the flux per dot would be $\sim 3 \times 10^{18}$ Mx. This may be compared with flux of 2.8×10^{18} Mx found at Kitt Peak.

An estimate of the dot density in regions of weak field can be made directly from counts: in 17 count areas where the Mount Wilson field measurement is $\leqslant 10$ G, the mean sum (the number of red dots + the number of blue dots) is 32 in 275 (arc s)^2 or 2.9 in 25 (arc s)^2. The mean difference, or number of uncompensated dots in these low-field regions, is 10 in 275 (arc s)^2 or 0.9 in 25 (arc s)^2.

Livingston and Harvey scanned near the center of the quiet solar disk using a Babcock-type magnetograph with aperture $5'' \times 5''$. When an isolated magnetic feature was detected, it was centered on the aperture, and the magnetic signal recorded. These signals tend to cluster at values that are multiples of 21 G, as can be seen in the observed histogram reproduced in Figure 4. The distribution within each signal range is skewed toward smaller values as would be expected, Livingston and Harvey point out, whenever inclination of the field direction or scattering beyond the aperture causes some loss of signal. Therefore, we consider all the cases with signal in the range 10 to 30 G to represent apertures containing a single element, those in the range 30 to 50 to contain 2 elements, etc. (Table I).

TABLE I

Livingston and Harvey's frequency distribution

Signal in gauss	10 to 30	30 to 50	50 to 70	70 to 90	90
Number of uncompensated magnetic elements	1	2	3	4	5
Number of cases observed	29	13	10	4	4

As the number of elements increases, the number of cases decreases only rather slowly, suggesting that more than one element must often fall into a single aperture area.

To determine the density of elements more precisely, we need to estimate the number of cases when the signal was zero, because either no elements, or equal numbers of positive and negative elements appeared in the aperture. As a trial estimate, we assume a binomial distribution for single elements. Suppose the elements fall into m surface areas, each $5'' \times 5''$. The probability that a certain area receive a given element is $p = 1/m \ll 1$. Let $1 - p = q \sim 1$. If there are n elements of each polarity, the number of areas containing 0, 1, 2, ..., j elements of + polarity will be proportional to

$$P_0 = q^n,\ P_1 = nq^{n-1}p,\ P_2 = (n(n-1)/2)\, q^{n-2}p^2,$$
$$\ldots,\ P_j = \frac{n!}{(n-j)!\, j!}\, q^{n-j}p^j, \ldots,$$

https://doi.org/10.1017/S0074180900022750 Published online by Cambridge University Press

and the same is true for − polarity. Then the number of cases with difference of 0, 1, 2,..., k between the number of + elements and the number of − elements will be proportional to the products of the probabilities, summed over all combinations that result in this difference.

$$D_0 = P_0P_0 + P_1P_1 + \cdots + P_nP_n$$

$$D_1 = 2\left[P_0P_1 + P_2P_3 + \cdots + P_jP_{j+1} \cdots + P_{n-1}P_n\right]$$

(both positive and negative differences are counted)

$$D_k = 2\sum_{0}^{n-k} P_jP_{j+k}\,.$$

The computation is simplified if we note that $n!/(n-j)! \sim n^j$, ignoring terms of order $1/n$ and smaller. Then

$$P_j \sim \frac{q^n}{j!}\left(\frac{np}{q}\right)^j = P_0\,\frac{xj}{j!},$$

where $x = np/q \sim n/m$ is approximately equal to the average number of elements of each polarity in one aperture area. The histograms in Figure 4 were constructed to fit these constraints: (1) the number of cases within each 20-G signal range is proportional to D_k defined above; (2) within each 20-G interval, the cases are distributed in the pattern 0.18, 0.23, 0.47, 0.12, the average pattern in Livingston and Harvey's distribution; (3) the number of cases with signal $\geqslant 10$ G, $\sum_{k=1}^{n} D_k$, is 60, as in the observed distribution. Some characteristics of each of the computed distributions are given in Table II.

TABLE II

Characteristics of the computed frequency distributions

$x = np/q$	1	1.7	2	2.5	3
Total number of cases for $N(\geqslant 1) = 60$	87	78	76	74	72
Total number of elements of each polarity	86	131	150	183	213
Density ($N^+ + N^-$)	2.0	3.4	4.0	5.0	5.9
Average excess, $N^+ - N^-$	1.0	1.4	1.5	1.7	1.9
Excess/sum	0.5	0.4	0.4	0.3	0.3

From the histograms and Table II we can estimate that a random distribution of elements that fits the observed distribution has x lying between 1.5 and 3.0, density between 3 and 6, average number of uncompensated elements between 1.3 and 1.9, and ratio of difference to sum between 0.3 and 0.4.

Table III summarizes the values derived from the two aspects of magnetic elements.

The values in Table III show that both sets of observations could fit into a single model of magnetic elements that are distributed almost randomly in quiet regions that are almost field-free on a large scale.

There are facts that make us doubt the reality of magnetic dots: (1) the possibility of

TABLE III

Comparison of characteristics derived from independent sources

	Kitt Peak	Lockheed
Element area, (arc s)^2	1	2
Density (number in $5'' \times 5''$)	3 to 6	3
Average excess	1 to 2	0.9
Average flux per element, maxwells	2.8×10^{18}	3×10^{18}

spurious effects arising in the photographic subtraction process; (2) the dots have not appeared in magnetograms with high spatial resolution in which both polarizations are recorded simultaneously, made at Aerospace Corporation's San Fernando Observatory; (3) the dots do not show up in Lockheed subtractions of frames exposed several minutes apart, although the lifetime of the dots would be expected to be much longer. Against these we can set the positive evidence: (1) the continuity of the appearance of the structure from thinly scattered dots through weak chains to strong chains that have the same appearance as the chromospheric network; (2) the correlation of dot excess with magnetic field measured with a scanning magnetometer; (3) sharing of characteristics such as density, size, and magnetic flux with elements observed at Kitt Peak.

References

Harvey, J. and Livingston, W.: 1969, *Solar Phys.* **10**, 283.
Livingston, W. and Harvey, J.: 1969, *Solar Phys.* **10**, 294.

Discussion

Pasachoff: After this week of discussing bright mottles and dark mottles, I would like to thank you for introducing us to red mottles and blue mottles at this penultimate moment.

You obviously have a lot of experience in making the color overlays, and I wonder if you could please comment on what happens when you move things slightly out of registration.

Sawyer: In fact, all the photographic work was done at Lockheed Observatory. However, I have seen misregistered material, and it has a rather disturbing appearance.

Leighton: In view of the fact that one cannot distinguish perfect cancellation within some very small offset, which could introduce a spurious 'grain' with subsequent cancellations, do you prefer to think of the effects as real or as spurious?

Sawyer: I believe that the effect is not simply due to offset, because that produces dark and bright elements in a fixed geometrical relationship, like bright peaks and shadows, at least in the same neighborhood; and the dots don't look like that. I tend to think of them as real, but rather on the basis of the agreement with the Kitt Peak observations.

Leighton: At one time I noticed that one often gets a spurious, grainy, second cancellation if the two singly-cancelled pictures are copied in too sharp focus. A truer result is obtained if these second-generation pictures are printed slightly out of focus.

Frazier: Did you check the noise of the whole system by cancelling a pair of filtergrams taken with the *same* polarity.

Smith, Sara: This has been done with other filter magnetograms, and a smooth background was obtained.

Title: I believe that it is possible to subtract pairs to $\pm 0.0005''$, if every process is carefully controlled. I have produced subtracted test movies on which displacements of $0.001''$ are detectable. However, one can produce any number if any part of the process is not under control.